ABSTRACT DATA

0187 VERDICT fIC correlation with prostate epithelial cell density versus clinical ADC

Marta Masramon Munoz, Manju Mathew, Thomy Mertzanidou, Joey Clemente, Adam Retter, Natasha Thorley, Lorna Smith, Francesco Grussu, Alistair Grey, Eoin Dineen, Greg Shaw, Dominic Patel, Lucy Caselton, Caroline Moore, David Atkinson, Aiman Haider, Alex Freeman, Daniel Alexander, Shonit Punwani, Eleftheria Panagiotaki

Clinical applications

Thursday, 3 15:30 – 17:00

Room: Exhibition hall

ABSTRACT

Summary:

Most types of prostate cancer are characterised by epithelial cell proliferation. This study examines the relationship between Apparent Diffusion Coefficient from multi-parametric MRI and intra-cellular volume fraction from VERDICT-MRI and histologically derived cell density and tissue fractions.

Introduction:

Histological examination is currently the gold standard for diagnosing prostate cancer (PCa). While multi-parametric MRI (mpMRI) offers a non-invasive alternative, its effectiveness in PCa diagnosis varies significantly among radiologists 1 due to the diverse morphology of PCa on MRI and the presence of confounding conditions like benign prostatic hyperplasia (BPH) 2, leading to potential diagnostic inaccuracies 3,4. MpMRI diagnosis strongly relies on the Apparent Diffusion Coefficient (ADC)5 despite confounding various histological changes. ADC has been investigated as a descriptor of cell density, with studies reporting correlations of r = -0.646, -0.61, 0.50 and -0.695 in several ROI-based analysis6–9.

The Vascular Extracellular and Restricted Diffusion for Cytometry in Tumours (VERDICT)-MRI framework uses a diffusion-weighted protocol and a biophysical tumour model to explain the diffusion signal10. Specifically, the intra-cellular volume fraction (fIC) parameter estimate from VERDICT demonstrates superior discrimination of clinically significant (cs) PCa compared to ADC maps from mpMRI 11–13 and offers improved identification of false positive lesions 14. Ex vivo validation studies reveal that regions with high fIC correspond to elevated histological cell density 15.

Here we analyse the relationship of in vivo VERDICT fIC with epithelial cell density maps obtained from prostatectomy histological specimens and compare against ADC. We employ personalized 3D-printed moulds of the prostate to obtain slice-to-slice correspondence between whole-mount histology slices from prostatectomy and corresponding in vivo VERDICT-MRI.

Methods:

Patient data. We analyse six patients from the Histo-MRI clinical trial (NCT04792138), where men suspected of PCa undergo mpMRI and VERDICT-MRI16. Images are acquired using a 3T scanner (Achieva, Ingenia; Philips Healthcare; Best; The Netherlands) and the pre-operative prostate MRI is used to 3D print personalised moulds. The prostate is placed in the mould, where guides are placed to aid the sectioning 17 . This ensures slice-to-slice correspondence between MR and histology images.

The sample presented correspond to patients with average age 64.5 +/- 5 years, PSA levels 9.5+/- 6 ng/mL and Gleason grades 3+4 (n=4), 3+4+5 (n=1) and 4+3 (n=1). Expert radiologists and histopathologists annotate cancerous regions of interest (ROIs) on the MRI (ADC from mpMRI and VERDICT fIC) and histology, respectively.

Epithelial cell density maps from histology. We use a custom pipeline (using QuPath software 18) to derive cell density maps from whole-mount histology, using a patch-based approach. We segment and count the number of nuclei in each 0.216 micro-meter2 patch. We segment the patches into stroma, lumen and epithelial tissue using a semiautomatic method (with Image Pro Premier (Media Cybernetics)19) as in 20–23. We weigh the cell density by the proportion of epithelial tissue.

Results:

Figure 1 shows a representative example of the derived parameter maps from histology, including the cell density, epithelial fraction, and epithelial cell density.

Figure 2 displays the benign and cancerous ROIs segmented in corresponding fIC and histological cell density maps. The images are horizontally flipped since they have not been aligned.

Figure 3 shows the resulting correlation plots between parameter maps from MRI (ADC and fIC) and histology (cell density, epithelial fraction, and epithelial cell density) using six samples. fIC is more strongly correlated to all histologically derived maps than ADC. fIC is

positively correlated to cell density, epithelial fraction, and epithelial cell density (r=0.6456,0.7769,0.6371) and ADC is negatively correlated (r=-0.3824,-0.6922,-0.4477). In both cases, the MR-derived maps correlate best with epithelial fraction.

Discussion & Conclusions:

This work presents a comparison of in vivo fIC maps from VERDICT-MRI and mpMRI ADC maps with corresponding histology parameter maps. Results show higher correlation between cell density and epithelial fraction with fIC (r=0.7769) than ADC (r=-0.6922) maps.
We obtain lower correlation between ADC and cell density than previous studies[6–9], possibly due to the small number of samples we use. We find that both ADC and fIC correlate better with epithelial fraction than cell density or epithelial cell density. This is concordant with histological changes in the prostate during the progression of adenocarcinoma, the most common type of prostate cancer, which is characterised by proliferation of epithelial cells[24,25].
This in vivo analysis of VERDICT fIC maps shows that the fIC compartment of the VERDICT model captures the contribution of epithelial cells in the prostate. It also shows that fIC is more specific to changes in epithelium than ADC. Future work will analyse more samples for statistical analysis and incorporate patch-by-patch analysis to better quantify the relationship between fIC and histologically derived measures.

References:

Ahmed, H. U. *et al.* Diagnostic accuracy of multi-parametric MRI and TRUS biopsy in prostate cancer (PROMIS): a paired validating confirmatory study. *The Lancet* **389**, 815–822 (2017).

Lovegrove, C. E. *et al.* Prostate imaging features that indicate benign or Malignant pathology on biopsy. *Translational Andrology and Urology* vol. 7 S420–S435 Preprint at https://doi.org/10.21037/tau.2018.07.06 (2018).

Rosenkrantz, A. B. *et al.* Interobserver reproducibility of the PI-RADS version 2 lexicon: A multicenter study of six experienced prostate radiologists. *Radiology* **280**, 793–804 (2016).

Westphalen, A. C. *et al.* Variability of the positive predictive value of PI-RADS for prostate MRI across 26 centers: Experience of the society of abdominal radiology prostate cancer disease-focused panel. *Radiology***296**, 76–84 (2020).

Wu, X. *et al.* Correlation between apparent diffusion coefficient value on diffusion-weighted MR imaging and Gleason score in prostate cancer. *Diagn Interv Imaging* **98**, 63–71 (2017).

Gibbs, P. *et al. Correlation of ADC and T2 Measurements With Cell Density in Prostate Cancer at 3.0 Tesla*. http://journals.lww.com/investigativeradiology (2009).

Zelhof, B. *et al.* Correlation of diffusion-weighted magnetic resonance data with cellularity in prostate cancer. *BJU Int* **103**, 883–888 (2009).

Glazer, D. I. *et al.* Diffusion-weighted endorectal MR imaging at 3T for prostate cancer: correlation with tumor cell density and percentage Gleason pattern on whole mount pathology. *Abdominal Radiology***42**, 918–925 (2017).

Xi, Z. W. *et al.* Diffusion-weighted imaging of prostate cancer: Correlation between apparent diffusion coefficient values and tumor proliferation. *Journal of Magnetic Resonance Imaging* **29**, 1360–1366 (2009).

Panagiotaki, E. *et al.* Noninvasive quantification of solid tumor microstructure using VERDICT MRI. *Cancer Res* **74**, 1902–1912 (2014).

Johnston, E. W. *et al.* VERDICT MRI for prostate cancer: Intracellular volume fraction versus apparent diffusion coefficient. *Radiology***291**, 391–397 (2019).

Singh, S. *et al.* Avoiding Unnecessary Biopsy after Multiparametric Prostate MRI with VERDICT Analysis: The INNOVATE Study. *Radiology* (2022) doi:10.1148/radiol.212536.

Appayya, M. B. *et al. The Intracellular Component of VERDICT (Vascular, Extracellular, and Restricted Diffusion for Cytometry in Tumors) MRI Distinguishes Gleason 4 Pattern Better than Apparent Diffusion Coefficient*. (2018).

Sen, S. *et al.* Differentiating False Positive Lesions from Clinically Significant Cancer and Normal Prostate Tissue Using VERDICT MRI and Other Diffusion Models. *Diagnostics* **12**, (2022).

Bailey, C. *et al.* VERDICT MRI validation in fresh and fixed prostate specimens using patient-specific moulds for histological and MR alignment. *NMR Biomed* **32**, (2019).

Singh, S. *et al.* Histo-MRI map study protocol: a prospective cohort study mapping MRI to histology for biomarker validation and prediction of prostate cancer. *BMJ Open* **12**, e059847 (2022).

Bourne, R. M. *et al.* Apparatus for histological validation of in vivo and ex vivo magnetic resonance imaging of the human prostate. *Front Oncol* **7**, (2017).

Bankhead, P. *et al.* QuPath: Open source software for digital pathology image analysis. *Sci Rep* **7**, (2017).

Media Cybernetics. Image-Pro. https://mediacy.com/image-pro/.

Chatterjee, A. *et al.* Changes in epithelium, stroma, and lumen space correlate more strongly with gleason pattern and are stronger predictors of prostate ADC changes than cellularity metrics1. *Radiology***277**, 751–762 (2015).

Chatterjee, A. *et al.* Validation of Prostate Tissue Composition by Using Hybrid Multidimensional MRI: Correlation with Histologic Findings. *Radiology* **302**, 368–377 (2022).

Lin, Y. *et al.* Diffusion radiomics analysis of intratumoral heterogeneity in a murine prostate cancer model following radiotherapy: Pixelwise correlation with histology. *Journal of Magnetic Resonance Imaging* **46**, 483–489 (2017).

Chatterjee, A. & Oto, A. Future Perspectives in Multiparametric Prostate MR Imaging. *Magn Reson Imaging Clin N Am* **27**, 117–130 (2019).

Eble JN, Sauter G, Epstein JI & Sesterhenn IA. *Tumours of the Urinary System and Male Genital Organs*. (IARC Press, 2004).

Epstein JI, Cubilla AL & Humphrey PA. *Tumors of the Prostate Gland, Seminal Vesicles, Penis, and Scrotum. AFIP Atlas of Tumor Pathology*. (American Registry of Pathology, 2011).

TABLES AND IMAGES

Figure 1

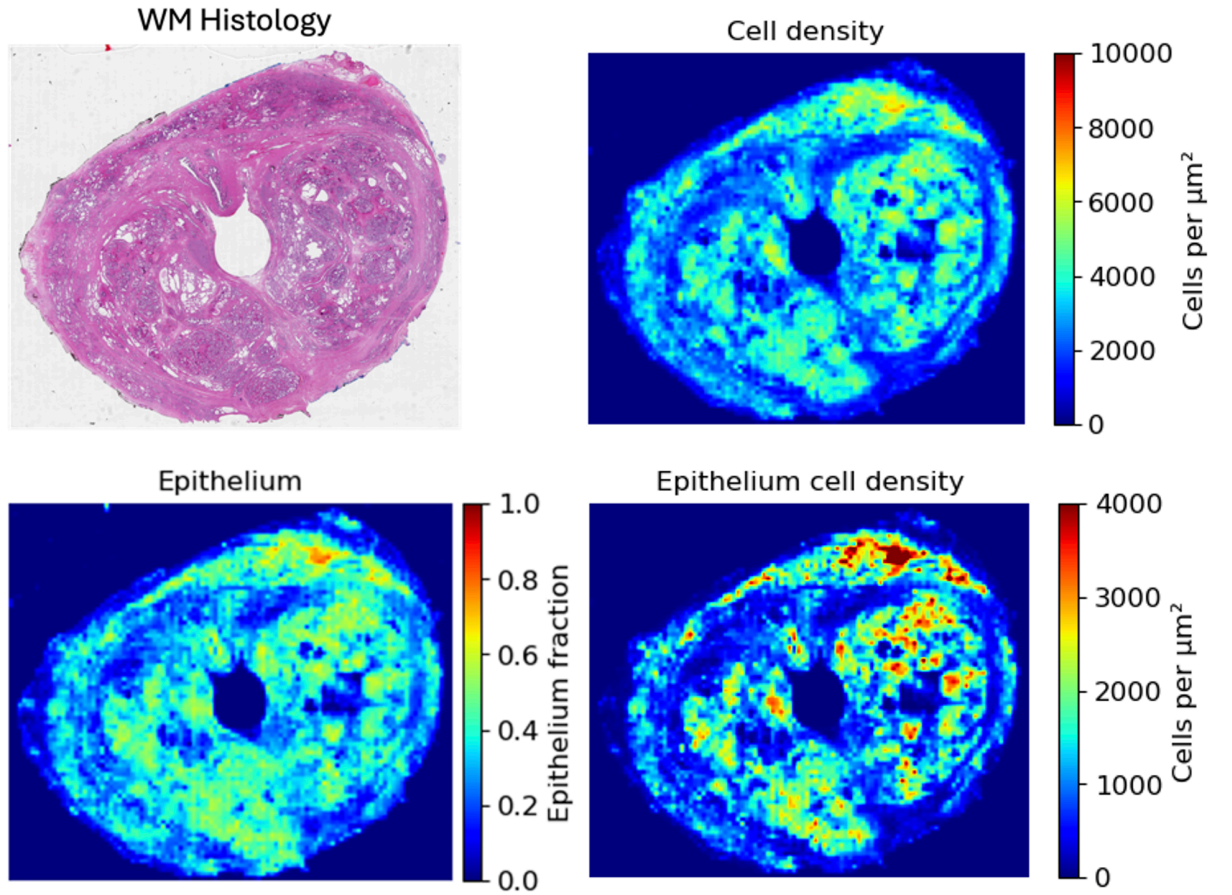

Example of derived histological maps from histology. The epithelium cell density is obtained by weighing the cell density with the epithelial tissue fraction.

Figure 2

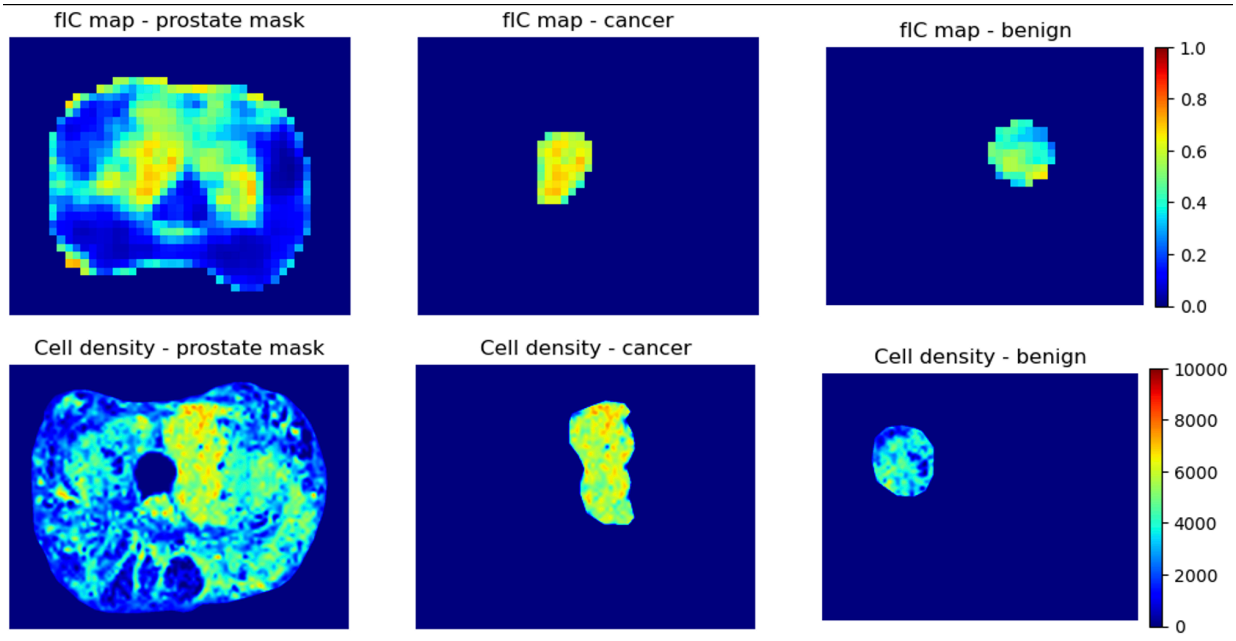

Example of corresponding ROIs in a fIC map from VERDICT-MRI and cell density map from histology. The images are not aligned - they differ by horizontal flipping.

Figure 3

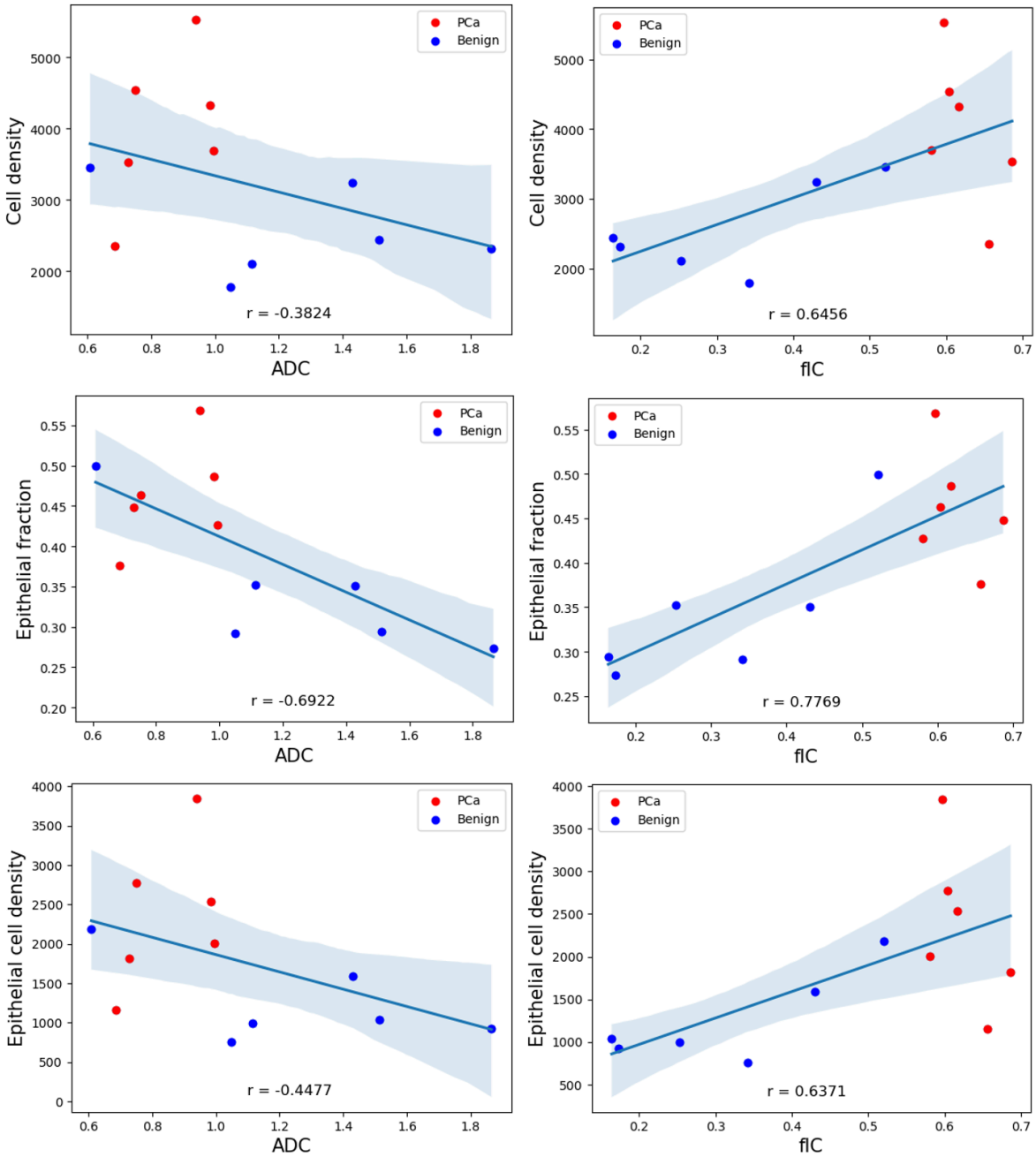

Correlations between average fIC/ADC values and histologically derived parameters in selected benign and cancerous ROIs. 95% confidence intervals are drawn in blue. R: Pearson's correlation coefficient.